Influence of thermochemical sulfate reduction on oxygen isotopic composition of calcite cements in carbonates of the Triassic Feixianguan and Permian Changxing formations in the Sichuan Basin, China

Guangwei Wang[1,2]*, Fang Hao[1,2], Huayao Zou[3] and Pingping Li[3]

[1]Shandong Provincial Key Laboratory of Deep Oil and Gas, China University of Petroleum (East China), Qingdao, China, [2]Laboratory for Marine Mineral Resources, Qingdao National Laboratory for Marine Science and Technology, Qingdao, China, [3]State Key Laboratory of Petroleum Resources and Prospecting, China University of Petroleum (Beijing), Beijing, China

Calcite cement is a common diagenetic mineral in carbonate rocks and plays an important role on rock quality as hydrocarbon reservoirs. Traditionally, oxygen isotopic compositions ($\delta^{18}O$) of the diagenetic calcites tend to decrease with increasing depths due to temperature-dependent isotope fractionation. In this study, the stable isotope compositions of the calcite cements in the Changxing and Feixianguan formations from the Puguang, Yuanba, Jiannan and Fuling carbonate fields in the Sichuan Basin were analyzed. The results show that some calcite cements have $\delta^{18}O$ values similar to those of their host carbonates, despite the fact that these calcites formed at elevated temperatures (>~100˚C). Based on petrographic and geochemical analyses, the ^{18}O-enriched calcites commonly occur with solid bitumens and have lower $\delta^{13}C$ values compared with host rocks, suggesting thermochemical sulfate reduction (TSR) provided organic carbon for these calcite precipitation. During TSR, thermal oxidation of hydrocarbons generated the light carbon, and simultaneously the reduced sulfate ions provided the oxygen. Comparison of our study with the TSR calcites worldwide, a model for oxygen isotope behavior during TSR was established. Oxygen isotope compositions of TSR-related calcites are a function of isotope compositions and amounts of the initial anhydrite and pore waters. TSR shows two opposing effects on the $\delta^{18}O$ values of calcites, depending on the $\delta^{18}O$ ratios of the initial anhydrite. The reduction of anhydrite with relatively low $\delta^{18}O$ values causes the calcite $\delta^{18}O$ lower than theoretical values of calcites directly precipitated from pore waters. The heavy $\delta^{18}O$ ratios of calcites formed during TSR are not only attributed to the ^{18}O-enriched pore water resulting from extensive water-rock interaction, but also probably due to the involvement of anhydrite with high $\delta^{18}O$ values.

Introduction

Calcite cementation is a common diagenetic event in sedimentary rocks that plays an important role in controlling reservoir quality (e.g., Schneidermann and Harris, 1985; Morad, 2009; Wang et al., 2017, 2022). It can take place under diverse diagenetic environments ranging from near surface through shallow to deep burial (Moore, 2001). The resultant calcite cements record fluid flow history in mineral textures and chemical and isotope compositions. This is especially true for the oxygen isotopic composition ($\delta^{18}O$), which is a function of the $\delta^{18}O_{water}$ and temperature of precipitating fluids, and thus serves as an important proxy for formation temperatures of minerals and their parent diagenetic fluids (Allan and Wiggins, 1993; Mangenot et al., 2018). For example, calcites precipitated from meteoric water commonly show relatively depleted $\delta^{18}O$ values compared to those from shallow-seawater that tend to have oxygen isotopic ratios similar to surrounding bulk-rocks (Allan and Wiggins, 1993; Machel et al., 1995). It is believed that calcite cements have more negative $\delta^{18}O$ values with increasing temperatures (Swart et al., 2016). The significant temperature-dependent isotopic fractionation can result in ^{18}O depletion in calcites with values overlapping those of meteoric waters, even if the calcite cements precipitated from pore waters with high $\delta^{18}O$ values (Moore, 2001). Thus, it appears that the oxygen isotopic composition of calcite cements is a combined result of the $\delta^{18}O$ and temperature of the parent fluid, overprinted by the temperature-dependent isotopic fractionation between mineral and fluid (Moore, 2001). However, the $\delta^{18}O$ may be influenced by other diagenetic reactions that were simultaneously providing oxygen involved in calcite precipitation. For example, calcite cements in organic-rich carbonates may have negative $\delta^{18}O$ values due to organic matter decomposition in the sulfate-reducing zone (Sass et al., 1991).

In the northeastern Sichuan Basin, the stable isotope compositions and fluid inclusions of the calcite cements and associated host-rock carbonates from the Upper Permian Changxing Formation (P_2ch) and the Lower Triassic Feixianguan Formation (T_1f) from the Puguang, Yuanba, Jiannan and Fuling carbonate gas fields (Figure 1) were analyzed. The $\delta^{18}O$ values of calcite cements display a wide range with the highest values similar to those of the host-carbonate rocks, despite the fact that these ^{18}O-enriched cements precipitated at much higher temperatures (commonly greater than 106°C). The relatively high $\delta^{18}O$ values of calcites are commonly attributed to formation at low temperature or from subsurface pore-waters that experienced extensive water-rock interaction (Heydari and Moore, 1989). In this study, we discuss the oxygen isotope behavior of the TSR-related calcites in the northeastern Sichuan Basin that is controlled by pre-existing pore water, as well as thermochemical sulfate reduction, a process that not only supplies light carbon, but also provides the oxygen for calcite precipitation at elevated temperatures.

Geological setting

The Upper Permian Changxing Formation and the Lower Triassic Feixianguan Formation are composed mostly of platform carbonates and are the two prolific gas-producing intervals in the northeastern Sichuan Basin (Ma et al., 2008; Zou et al., 2008). The Sichuan Basin is located in the southwestern China (Figure 1). It is bounded to the west by the Longmenshan Fold Belt, to the north by the Micangshan Uplift and the Dabashan Fold Belt, to the southeast by the Hubei-Hunan-Guizhou Fold Belt, and by the Emeishan-Liangshan Fold Belt to the southwest. Deposition started in the Cryogenian period and a total of more than 10 km of sediments were laid down on the metamorphic basement of the Yangtze Paraplatform during the Jinning and Chengjiang orogenies (Figure 2; Ma et al., 2008).

Due to the rapid local subsidence of the basement during the early Changxing period, the Kaijiang-Liangping Trough formed and prevailed until the later stage of the Feixianguan period, which resulted in a semi-isolated platform to the east separated from a broad platform to the west (Figure 1; Wei et al., 2004). During the Changxing period, the reef and bioclastic shoals prevailed within the platform, which were subsequent pervasively dolomitized in the Puguang and Yuanba gas fields. During the Feixianguan period, oolitic shoals were present on two margins of the platform. The shoals on the western platform are mainly composed of limestones with very limited dolostones in the Yuanba and Fuling carbonate gas fields, while those on the eastern semi-isolated platform were mainly dolostones in the Puguang gas field. Subsequently, abundant anhydrites of the Lower Triassic Jialingjiang Formation and the Middle Triassic Leikoupo Formation served as regional cap rocks.

Reconstruction of the burial and thermal histories shows that the Changxing and Feixianguan carbonate reservoirs in these four gas fields experienced maximum temperatures greater than 140°C which is regarded as a critical temperature above which TSR begins. Detailedly, the Feixianguan carbonates in the Puguang gas field were buried to a depth of about 7,000 m and experienced maximum temperature up to 220°C before uplifted (Hao et al., 2015), while in the Jiannan area they were buried to a maximum depth of approximately 6,900 m and experienced temperatures up to 195°C before having been uplift to the present-day depths of 3,000–4,000 m (Wang et al., 2015b). The Changxing carbonate reservoirs in the Yuanba gas
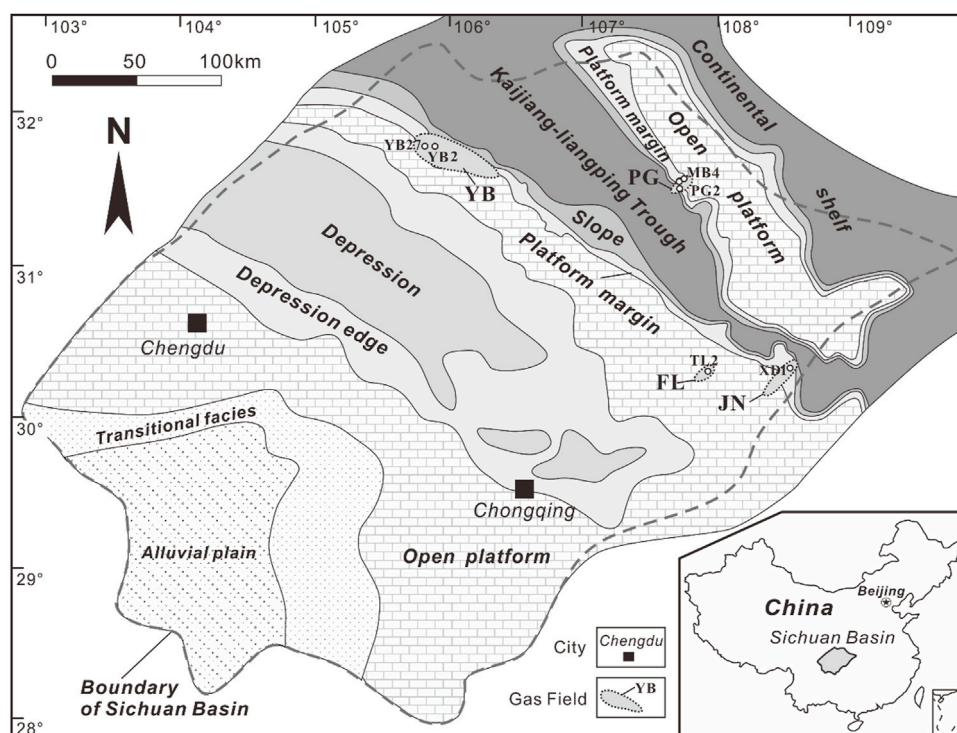
FIGURE 1
Sedimentary facies during the deposition of the Changxing Formation in the Sichuan Basin showing the distribution of the wells in each of the gas fields (from Li et al., 2016). PG = Puguang; YB = Yuanba; FL = Fuling; JN = Jiannan.

field reached maximum burial depths of approximately 8,000 m and temperatures of approximately 240°C during the Late Cretaceous (Li et al., 2016). The Changxing carbonates in the Fuling gas field reached maximum burial depths of approximately 8,000 m and temperatures of approximately 215°C during the Middle Cretaceous.

Hydrocarbon gases in the Puguang, Yuanba, Fuling and Jiannan gas fields are mainly produced from the P_2ch and T_1f carbonate reservoirs. The gases from the Feixianguan limestone reservoirs in the Yuanba gas field are composed of very low H_2S concentrations commonly less than 1%, while gases from Feixianguan Formation in the Puguang gas field and the Changxing Formation in the Yuanba gas field commonly have high H_2S concentrations (Cai et al., 2003; Li et al., 2016). In the Fuling gas field, samples were taken from the Permian Changxing dolomitic limestone intervals of the TL2 well, and the concentration of H_2S is 13.6%.

Samples and methods

All samples used in this study are from well cores. Samples analyzed from the Yuanba and Puguang gas fields were from the Feixianguan limestone reservoirs. Samples from the Fuling gas field were collected from the Changxing limestone reservoirs from TL2 well cored intervals. Double-polished thin sections were prepared and examined under cathodoluminescence using an Mk5-2 stage operating at 280 μA and 13 kV in Shandong Provincial Key Laboratory of Deep Oil & Gas, China University of Petroleum (East China), Qingdao. A total of 61 samples were selected for carbon and oxygen isotope analysis. The host carbonate rocks and calcite nodules were directly powered using an agate mortar and pestle to less than 200 mesh, while pore-filling calcite cements were collected by micro-sampling techniques (Fouke and Rakovan, 2001) at the China University of Geosciences, Wuhan. Double-polished thin sections were placed under stereomicroscope and calcite powers were extracted using a low speed micromill drill assembly that were then collected (~20 μg) by a micropipette tip. Stable carbon and oxygen isotope rations were measured in the State Key Laboratory of Geological Processes and Mineral Resources in China University of Geosciences. Calcite powders were reacted in a Thermo-Scientific Kiel IV automated carbonate device with 100% pure phosphoric acid to generate CO_2 gas that was subsequently analyzed on a Finnigan MAT-253 mass. Analytical precisions are generally better than 0.1‰ for $\delta^{18}O$, and better than 0.05‰ for $\delta^{13}C$, respectively. The values for the carbon and oxygen isotope are reported in parts per thousand (‰) relative to the

FIGURE 2

Chronostratigraphy		Lithostratigraphy		Lithology	Thickness (m)	Depositional Environment	Tectonic Movement
		Formation	Code				
Quaternary			Q				Late Himalayan
Neogene			Ng				
Paleogene			Pg				Early Himalayan
Cretaceous			K				LateYanshanian
Jurassic	Upper	Penglaizhen	J3p		>650	Alluvial-lucustrine facies sandstones, mudstones and shale	
		Suining	J3sn				
	Middle	Shaximiao	J2s		~2000		Early Yanshanian
	Lower	Ziliujing	J1z		~760		
Triassic	Upper	Xujiahe	T3x		~200	Marine carbonates, evaporites and black shale and alternating marine and terrestrial facies clastics and coal-bearing buildup	Late Indosinian
	Middle	Badong	T2b		~550		Early Indosinian
	Lower	Jialingjiang	T1j		~950		
		Feixianguan	T1f		~400		
Permian	Upper	Changxing	P2ch		~330		Dongwu
		Wujiaping	P2w				
	Lower	Maokou	P1m		~400		
		Qixia	P1q				
		Liangshan	P1l				Yunnan
Carboniferous		Huanglong	C2h		~40		Caledonian
Devonian			D		~20		Guangxi
Silurian	Middle	Hanjiadian	S2h		~1230		
	Lower	Xiaoheba	S1x				
		Longmaxi	S1l				
Ordovician			O		~360		
Cambrian			Є		~1800		
Ediacaran		Dengying			300~2500		Tongwan
		Doushantuo					Chengjiang
Cryogenian							Jinning
Pre-Cryogenian		Basement				Basement	

Legend: Shale, Shaly Siltstone, Sandstone, Limestone, Oolitic Grainstone, Marly Limestone, Dolomite, Reef Dolomite, Bioclastic Dolomite, Marly Dolomite, Anhydrite, Metamorphosed Basement
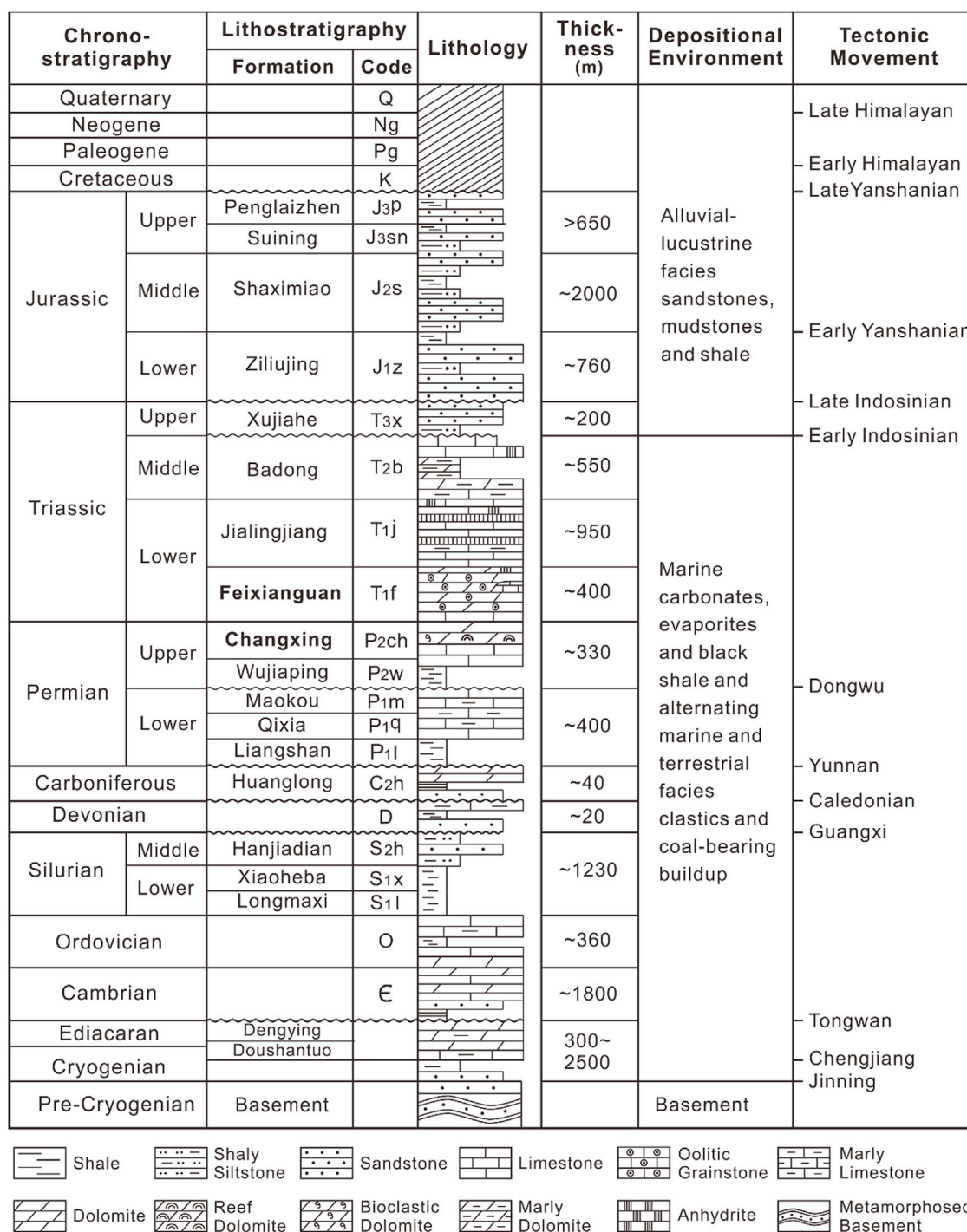
Generalized stratigraphy and tectonic history of the NE Sichuan Basin (from Wang et al., 2015).

Vienna Peedee Belemnite (V-PDB). For measurement of $\delta^{18}O$, ten anhydrite samples were also analyzed on a Finnigan MAT-253 mass spectrometer at the Center for Geological Analysis and Testing, Beijing Institute of Geology, Nuclear Industry.

Observation and microthermometry of fluid inclusions in calcites were conducted on eight samples. Microthermometric measurements of homogenization temperatures (T_h) were performed on primary two-phase (liquid and vapour) fluid
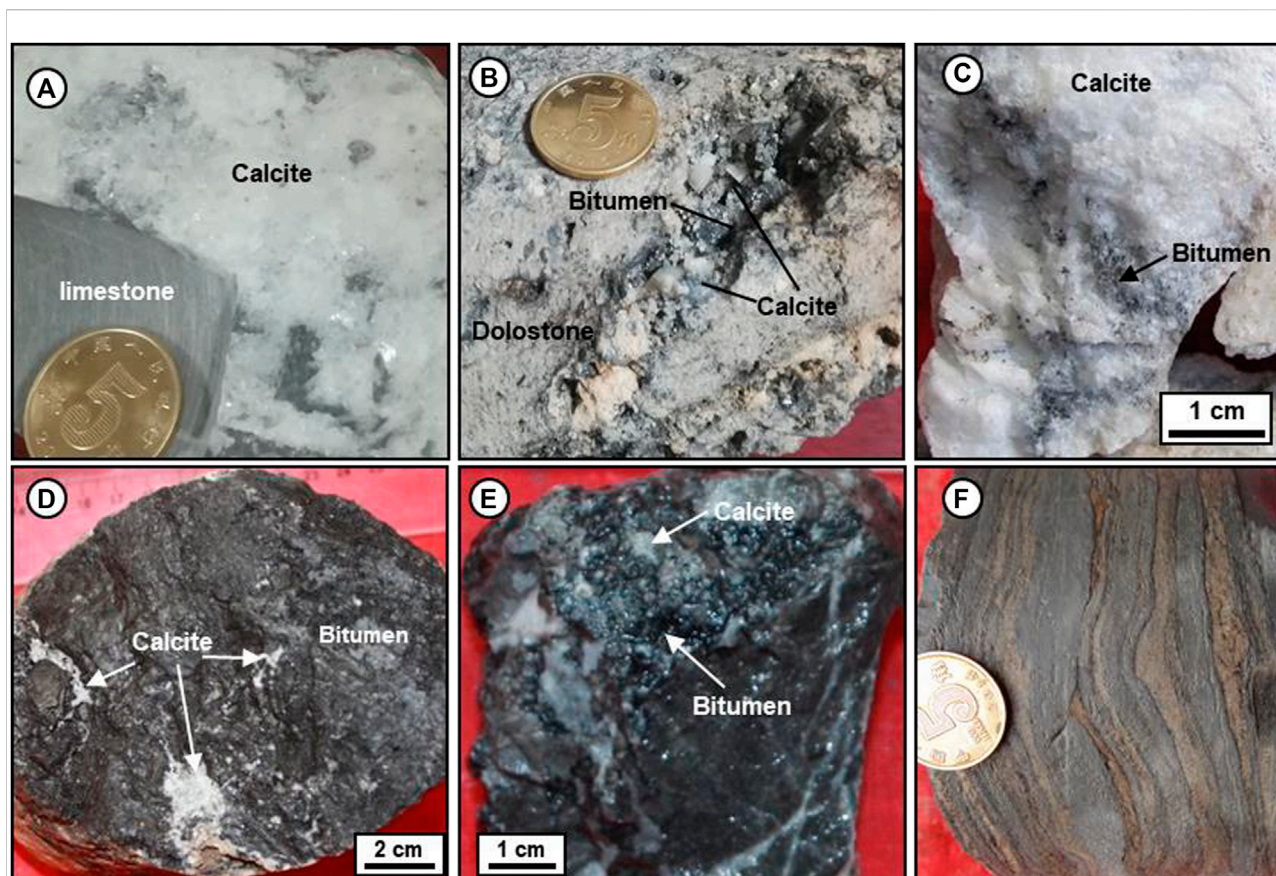
FIGURE 3
Photographs of well cores showing typical calcite cements from the Upper Changxing and the Lower Feixianguan formations, northeastern Sichuan Basin. **(A)** Calcite cement filling in the micro-fracture without solid bitumen. TL2 well in the Fuling gas field, 5237.43 m. **(B)** Calcites occurred as coalescing euhedral crystals with solid bitumens in vugs of dolostones, MB3 well, 4393.22 m. **(C)** Nodule calcites with solid bitumens. XD1 well, 3260.41 m **(D, E)** Calcites occurred with solid bitumen reflecting post-oil charge origin. TL2 well, 5235.92 m and 5236.03 m. **(F)** The TSR-related calcites that partially replaced anhydrite. (Details can be found in Figures 4). MB3 well, 3884.99 m.

inclusions using a Linkam THMSG600 heating and freezing stage coupled with Linksys 32 software. The repeated T_h value for the same fluid inclusion is generally reproducible to within ±1.0°C.

Results

Petrographic characteristics

In the northeastern Sichuan Basin, calcite cements observed in the Upper Permian Changxing Formation and in the Lower Triassic Feixianguan Formation include early isopachous fibrous calcites and burial calcites. The fibrous calcites are isopachous (Figure 4A), and usually occur as the first generation of cements around grains, which is the characteristics of a shallow marine origin (Wang et al., 2015b). In this study, we focus on the burial calcite cements that usually occur as fillings in pores, vugs, or fractures, and are also present as nodules that probably replaced

anhydrite and coalescing euhedral crystals (Figures 3, 4). In the northeastern Sichuan Basin, abundant solid bitumens, generated from *in situ* cracking of crude oil accumulated in carbonate reservoirs (Zou et al., 2008; Hao et al., 2009), were found in well cores and thin sections in the Feixianguan and Changxing formations. Thus, these burial calcite cements can be subdivided into pre-TSR calcite and TSR calcite based on the relative timing of calcite precipitation compared to oil charging or solid bitumen, as well as oxygen and carbon stable isotopic compositions.

The pre-TSR calcites occur as pore and fracture-fillings that grew directly from the substrate surfaces of fractures (Figure 3A) and pores (Figure 4A) are often lined by early marine fibrous cements. These calcite cements may completely fill the pores without solid bitumens (Figures 4A,C). The residual pores, if present, were subsequently occluded by solid bitumens (Figure 4A). Under cathodoluminescence (CL), the pre-oil charge calcites display no to very weak dull red CL (Figures
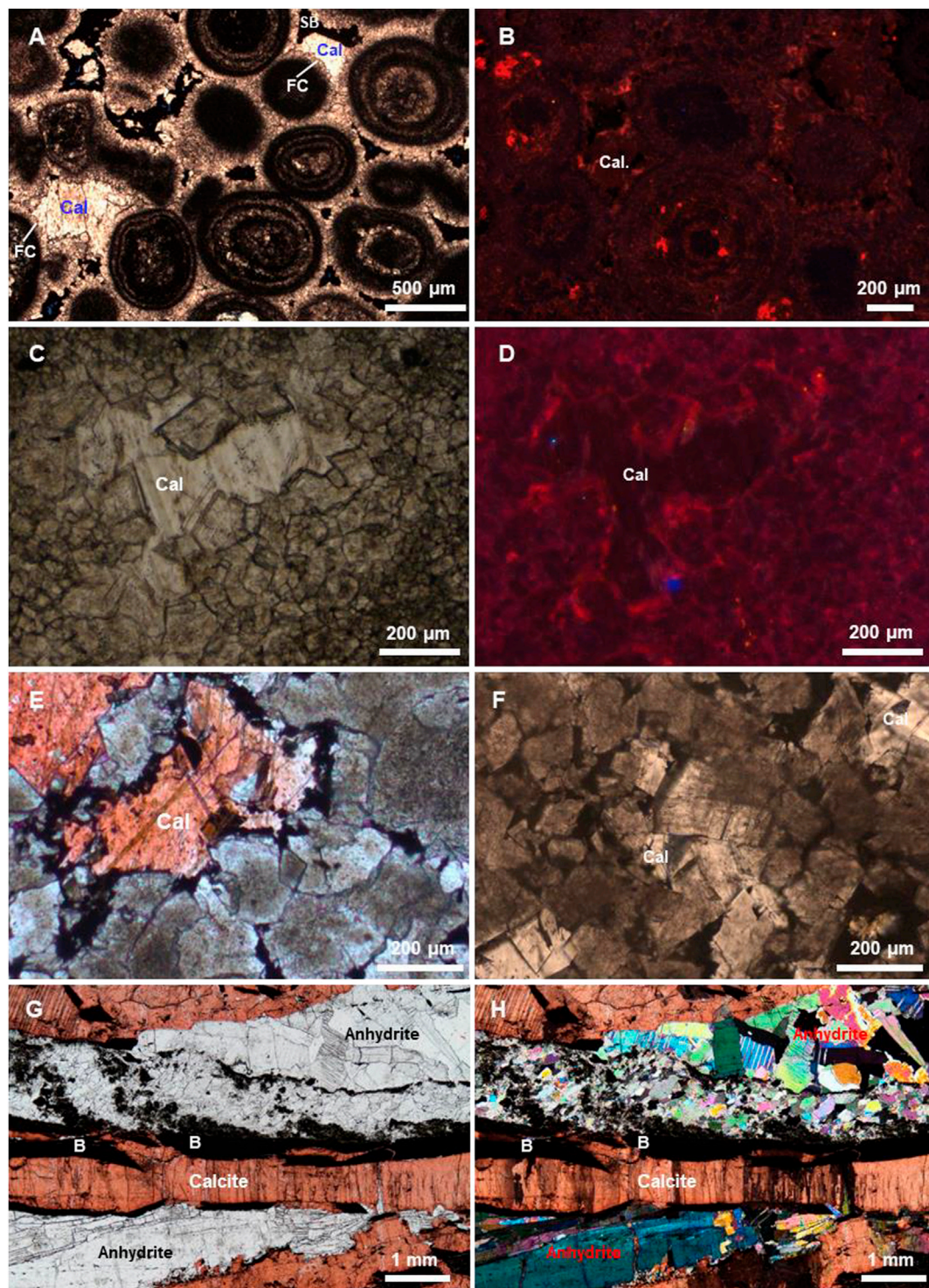
FIGURE 4
Photomicrographs showing the typical characteristics of the calcite cements from the Changxing and Feixianguan formations in the northeast Sichuan Basin. **(A)** Pre-TSR blocky calcites (Cal) filling in intergranular pores of grainstone which are lined by fibrous calcites (FC). The residual pores were completely occluded by solid bitumens (SB). YB21 well, 6665.11 m, Yuanba gas field. **(B)** Intergranular pore-filling pre-TSR calcites (Cal) showing no CL, YB27 well, 6126.89 m, Yuanba gas field. **(C, D)** Pre-TSR calcites (Cal) filling in intergranular pores of dolostone showing weakly dull red cathodoluminescence (CL). MB4 well, 3827.09 m, Puguang gas field. **(E)** TSR-related calcites (Cal) growing from solid bitumen-coated pores. PG2 well, 4935.5 m, Puguang gas field (Hao et al., 2015). **(F)** TSR-related calcites in pores of dolostone with solid bitumen. L8 well, 3831.44 m, Jiannan gas field. **(G, H)** TSR-related calcites that replaced anhydrite. Note many solid bitumens occur. MB3 well, 3884.99 m, Puguang gas field.
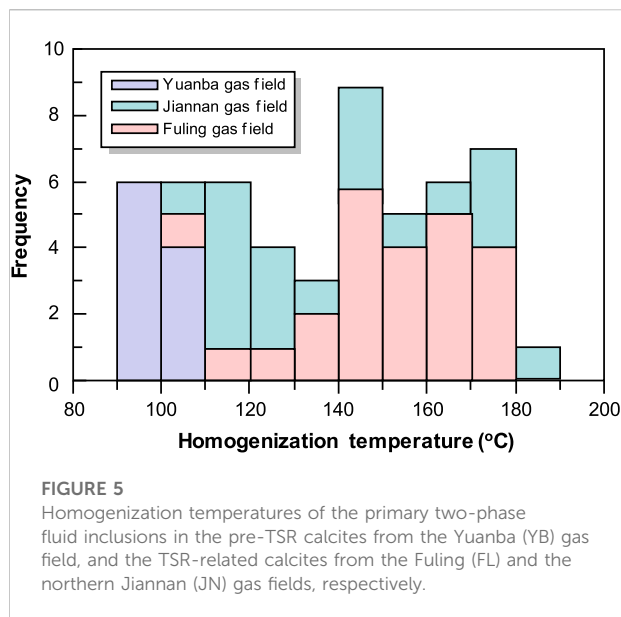
FIGURE 5
Homogenization temperatures of the primary two-phase fluid inclusions in the pre-TSR calcites from the Yuanba (YB) gas field, and the TSR-related calcites from the Fuling (FL) and the northern Jiannan (JN) gas fields, respectively.

Stable isotope compositions

Results of stable carbon and oxygen isotope compositions of the calcite cements and associated host rocks in the northeastern Sichuan Basin are summarized in Table 1 and shown in Figure 6. The host-rock dolostones from the Puguang gas field have $\delta^{13}C$ values ranging from 1.4‰ to 3.1‰ (average value of 2.3‰) and the $\delta^{18}O$ values from -6.1‰ to -4.4‰ (average value of -5.4‰). The pre-TSR cements have a narrow range of $\delta^{13}C$ values from 1.3‰ to 2.7‰ (except one at -1.3‰ due likely to a mixed calcite sample) with $\delta^{18}O$ values decreasing from-8.6‰ to -6.0‰ (Trend I in Figure 6A). In contrast, the post-oil charge cements show $\delta^{13}C$ values decreasing from-13.8‰ to -1.9‰ (Trend II in Figure 6A) and have $\delta^{18}O$ values from -7.3‰ to -5.5‰.

In the Yuanba gas field, the host-rock limestone from the Feixianguan Formation has an average $\delta^{13}C$ value of 1.9‰ (ranging from 1.4 ~2.3‰) and an average $\delta^{18}O$ value of -6.2‰ (ranging from -6.4~-6.0‰), while the pre-TSR calcites has the similar average $\delta^{13}C$ value of 1.9‰ (ranging from 1.8 ~2.0‰) but the slightly depleted $\delta^{18}O$ value of -7.2‰ (ranging from -7.1~-7.3‰, Trend I in Figure 6B). No TSR-related calcites are observed from the Feixianguan carbonates in this gas field.

The stable isotope rations for these calcites from the Fuling gas field exhibit two trends (Figure 6C). The host limestone rocks have $\delta^{13}C$ values in range from 4.1 to 4.3‰ with a mean value of 4.2‰ and the $\delta^{18}O$ values from -6.2‰ to -6.0‰ with a mean value of -6.1‰. The pre-TSR calcites have the $\delta^{13}C$ values of 3.9‰–4.2‰ (a mean value of 4.0‰), similar to the host rocks, and the lighter $\delta^{18}O$ values from -8.7 to -6.9‰ (mean value of -7.8‰) relative to the host rocks. In contrast, compared to the host rocks, the TSR-related calcites have the lighter $\delta^{13}C$ values of 3.1‰–3.2‰ (a mean value of 3.2‰) and the similar $\delta^{18}O$ values from -6.07 to -6.12‰ (average value of -6.1‰).

The host-rock dolostones from the XD1 well in the Jiannan gas field have the $\delta^{13}C$ values ranging from 4.1‰ to 4.7‰ (average value of 4.4‰) and the $\delta^{18}O$ values from -7.2‰ to -6.2‰ (average value of -6.7‰), while the two calcite cements have the same $\delta^{13}C$ values of 2.7‰ with $\delta^{18}O$ values from -7.1 to -6.9‰ (average value of -7.0‰, Trend II in Figure 6D), similar to the host rocks. No pre-TSR calcites were analyzed in this gas field.

A total of ten anhydrite samples from the Feixianguan dolostones from the XHC1, MB1, and MB3 wells in the northeastern Sichuan Basin have the $\delta^{18}O$ values from 16.4‰ to 23.1‰ SMOW with an average value of 18.6‰ SMOW.

4B,D). In the Jiannan gas field, these burial calcites form after dolomite formation (Figure 4C) which has been proposed to be burial origin (Wang et al., 2015a), while the burial calcites form obviously prior to marine fibrous calcite cementation in the Yuanba gas field (Figure 4A). The T_h values of the primary fluid inclusions hosted in pre-TSR calcites exhibit a range of temperature from 83.6°C to 103.2°C (Figure 5), also confirming their burial origin.

Although it is difficult to determine the formation timing of some calcites based on diagenetic sequence, the TSR-related calcites in this study are identified according to the combined evidences of the petrographic features, carbon isotopic compositions, and the homogenization temperatures of primary fluid inclusions. Generally, the TSR-related calcites in the northeastern Sichuan Basin are commonly accompanied with solid bitumens, and have much lighter carbon isotopic compositions compare to host rocks. In hand specimens, they occur as coalescing euhedral crystals in vugs (Figure 3B), isolated nodules containing solid bitumens (Figures 3C–E), and the calcites that replaced anhydrite (Figure 3F). Under the microscope, the typical feature of the TSR-related calcites is that the calcite crystals grew from bitumen-coated grain surfaces (Figures 4E,F). In addition, calcites that replaced anhydrite during TSR commonly occur with abundant solid bitumen (Figures 4G,H). Additionally, the T_h values of fluid inclusions in the post-oil calcites exhibit a wide range from 106.8°C to 183.9°C (Figure 5), probably reflecting a continuous precipitation during progressive burial.

TABLE 1 The oxygen and carbon isotope compositions of the pre-oil charging calcite, post-oil charging calcites and surrounding host carbonate rocks in the Changxing and Feixianguan formations in the northeast Sichuan Basin.

Location	No.	Wells	Lithology	$\delta^{18}O$ (‰)	$\delta^{13}C$ (‰)	Formation	Depth (m)
Puguang gas field	1	PG1	dolostone	-5.5	2.5	T1f	5423.70
	2	PG2	dolostone	-6.1	3.1	T1f	4778.69
	3	PG8	dolostone	-5.4	2.4	T1f	5532.30
	4	PG12	dolostone	-5.1	2.0	T1f	6004.10
	5	PG12	dolostone	-5.6	2.2	T1f	6005.10
	6	PG12	dolostone	-5.2	2.2	T1f	6005.15
	7	PG12	dolostone	-5.4	2.3	T1f	6005.63
	8	PG12	Lime dolostone	-5.6	2.3	T1f	6008.65
	9	MB3	dolostone	-5.5	2.3	P2ch	4334.30
	10	MB3	dolostone	-5.5	2.5	P2ch	4384.60
	11	MB3	dolostone	-5.6	1.4	P2ch	4415.64
	12	MB4	dolostone	-4.4	2.6	T1f	3856.69
	13	MB4	dolostone	-4.4	2.2	T1f	3856.84
	14	MB4	dolostone	-5.5	2.3	T1f	3856.99
	15	MB4	dolostone	-5.7	2.1	T1f	3857.54
	16	MB4	dolostone	-5.8	2.3	T1f	3858.24
	17	PG1	pore-filling calcite	-6.8	1.5	T1f	5423.70
	18	PG2	pore-filling calcite	-7.6	1.3	T1f	4825.70
	19	PG2	pore-filling calcite	-6.6	2.7	T1f	4778.69
	20	PG2	pore-filling calcite	-6.4	2.2	T1f	4778.69
	21	PG7	pore-filling calcite	-6.7	1.8	T1f	5614.13
	22	PG8	calcite in vug	-8.6	-1.3	T1f	5532.30
	23	PG10	pore-filling calcite	-6.4	2.5	T1f	6111.36
	24	PG12	pore-filling calcite	-6.7	1.3	T1f	6005.10
	25	PG12	pore-filling calcite	-6.8	1.4	T1f	6005.15
	26	PG12	pore-filling calcite	-6.0	1.7	T1f	6005.63
	27	PG12	pore-filling calcite	-6.8	1.6	T1f	6008.65
	28	MB3	calcite with anhydrite	-7.3	-13.8	T1f	3884.99
	29	MB3	calcite nodule	-6.4	-12.6	P2ch	4334.30
	30	MB3	pore-filling calcite	-5.9	-2.1	P2ch	4392.25
	31	MB3	calcite nodule	-5.5	-1.9	P2ch	4392.25
	32	MB3	calcite nodule	-5.9	-10.0	P2ch	4415.64
	33	MB4	pore-filling calcite	-6.6	1.4	T1f	3827.09
	34	MB4	pore-filling calcite	-6.0	1.8	T1f	3856.50
	35	MB4	pore-filling calcite	-6.0	1.9	T1f	3856.84
	36	MB4	pore-filling calcite	-7.0	1.4	T1f	3856.99
	37	MB4	pore-filling calcite	-7.0	1.5	T1f	3857.54
	38	MB4	pore-filling calcite	-7.7	1.4	T1f	3858.24
Fuling gas field	39	TL2	Limestone	-6.0	4.1	P2ch	5235.92
	40	TL2	Limestone	-6.1	4.3	P2ch	5236.85
	41	TL2	Limestone	-6.2	4.3	P2ch	5237.43
	42	TL2	Limestone	-6.1	4.3	P2ch	5238.11
	43	TL2	calcite with solid bitumen	-6.1	3.1	P2ch	5235.92
	44	TL2	calcite with solid bitumen	-6.1	3.2	P2ch	5236.03
	45	TL2	fracture-filling calcite	-8.7	4.2	P2ch	5236.85
	46	TL2	fracture-filling calcite	-7.7	3.9	P2ch	5237.43
	47	TL2	fracture-filling calcite	-6.9	4.0	P2ch	5238.11

TABLE 1 (*Continued*) The oxygen and carbon isotope compositions of the pre-oil charging calcite, post-oil charging calcites and surrounding host carbonate rocks in the Changxing and Feixianguan formations in the northeast Sichuan Basin.

Location	No.	Wells	Lithology	δ^{18}O (‰)	δ^{13}C (‰)	Formation	Depth (m)
Jiannan gas field	48	XD1	dolostone	-6.8	4.3	T1f	3259.51
	49	XD1	dolostone	-7.2	4.2	T1f	3261.41
	50	XD1	dolostone	-7.1	4.1	T1f	3262.21
	51	XD1	dolostone	-6.2	4.7	T1f	3263.71
	52	XD1	dolostone	-6.3	4.6	T1f	3267.10
	53	XD1	calcite nodule	-6.9	2.7	T1f	3260.41
	54	XD1	calcite nodule	-7.1	2.7	T1f	3262.21
Yuanba gas field	55	YB2	Limestone	-6.3	1.4	T1f	6401.02
	56	YB2	Limestone	-6.4	1.9	T1f	6428.61
	57	YB2	Limestone	-6.2	2.1	T1f	6429.36
	58	YB2	Limestone	-6.1	1.9	T1f	6455.11
	59	YB2	Limestone	-6.0	2.3	T1f	6459.02
	60	YB2	Pore-filling calcite	-7.3	2.0	T1f	6459.02
	61	YB2	Pore-filling calcite	-7.1	1.8	T1f	6455.11

Discussion

Origin of the heavy oxygen isotope compositions

The oxygen isotope compositions of calcites provide important information for reconstruction of diagenetic environments (Allan and Wiggins, 1993) as they are generally controlled by the nature of parent fluids and the temperatures of calcite precipitation (Moore, 2001). In the northeastern Sichuan Basin, the calcite cements exhibit two distinct trends in carbon and oxygen isotope compositions when compared to the host-rock carbonates (Figure 6). One trend (refer to as Trend I) is defined by calcite samples that have relatively scattered δ^{18}O values but show a very narrow range of the δ^{13}C values, similar to those of the surrounding host rocks. Another trend (refer to as Trend II) is evident by the calcite samples that show relatively lighter δ^{13}C values with most δ^{18}O values close to or partly overlapped with those of the host rocks.

Trend I is observed in the calcites from the Puguang, Yuanba, and Fuling gas fields (Figures 6A–C), as well as the Smackover Formation (Figure 6E from Heydari and Moore, 1989). These calcite cements are generally characterized by the precipitation prior to oil charging. The oxygen isotope compositions of the pre-TSR calcites are depleted in various degrees relative to those of the host carbonate rocks. This may be related to processes, such as temperature-dependent isotopic fractionation at high precipitation temperatures or the involvement of meteoric water with low δ^{18}O values. The relatively high T_h values of primary fluid inclusions in these calcites indicate formation in deep burial environments, exclude the influx of low-temperature meteoric water. Even though meteoric water could penetrate into deep

burial, it would be enriched in ^{18}O by water-rock interaction during migration (Machel et al., 1995). Therefore, the lower δ^{18}O ratios of the pre-TSR calcites are most likely attributed to the higher precipitation temperatures compared with host rocks. Furthermore, the variation in the oxygen isotope compositions of these calcite cements resulted from different precipitation temperatures with the δ^{18}O trend toward depleted values reflecting precipitation at higher temperatures during progressive burial (Heydari and Moore, 1989). The carbon isotope compositions of the pre-TSR calcite cements are identical to those of host-rock carbonates in each gas field, which suggests that the carbon in calcites was mainly sourced from or buffered by the host rocks.

A particular phenomenon observed is the trend II in the TSR-related calcites from the Puguang, Fuling, and Jiannan gas fields (Figures 6A,C,D). The T_h values of primary fluid inclusions in these calcites are commonly greater than 106°C (Figure 5), obviously higher than the pre-TSR calcite cements. The TSR-related calcites have heavier oxygen isotopic ratios than pre-TSR calcites. This is incompatible with the conventional model of the temperature-dependent oxygen isotopic fractionation that the calcite cements precipitated at higher temperatures have depleted δ^{18}O values compared to those precipitated at low temperatures. The relatively higher δ^{18}O values of the TSR-related calcites may be due to several processes.

The first possibility is the involvement of fluids with heavy oxygen isotope compositions for calcite precipitation. Such fluids could be formed during progressive burial due to extensive carbonate-water interaction because of preferentially incorporation of ^{16}O in solid phase, enhancing more ^{18}O residue in fluid phase, such as δ^{18}O values of pore waters from the Smackover Formation at burial depths of
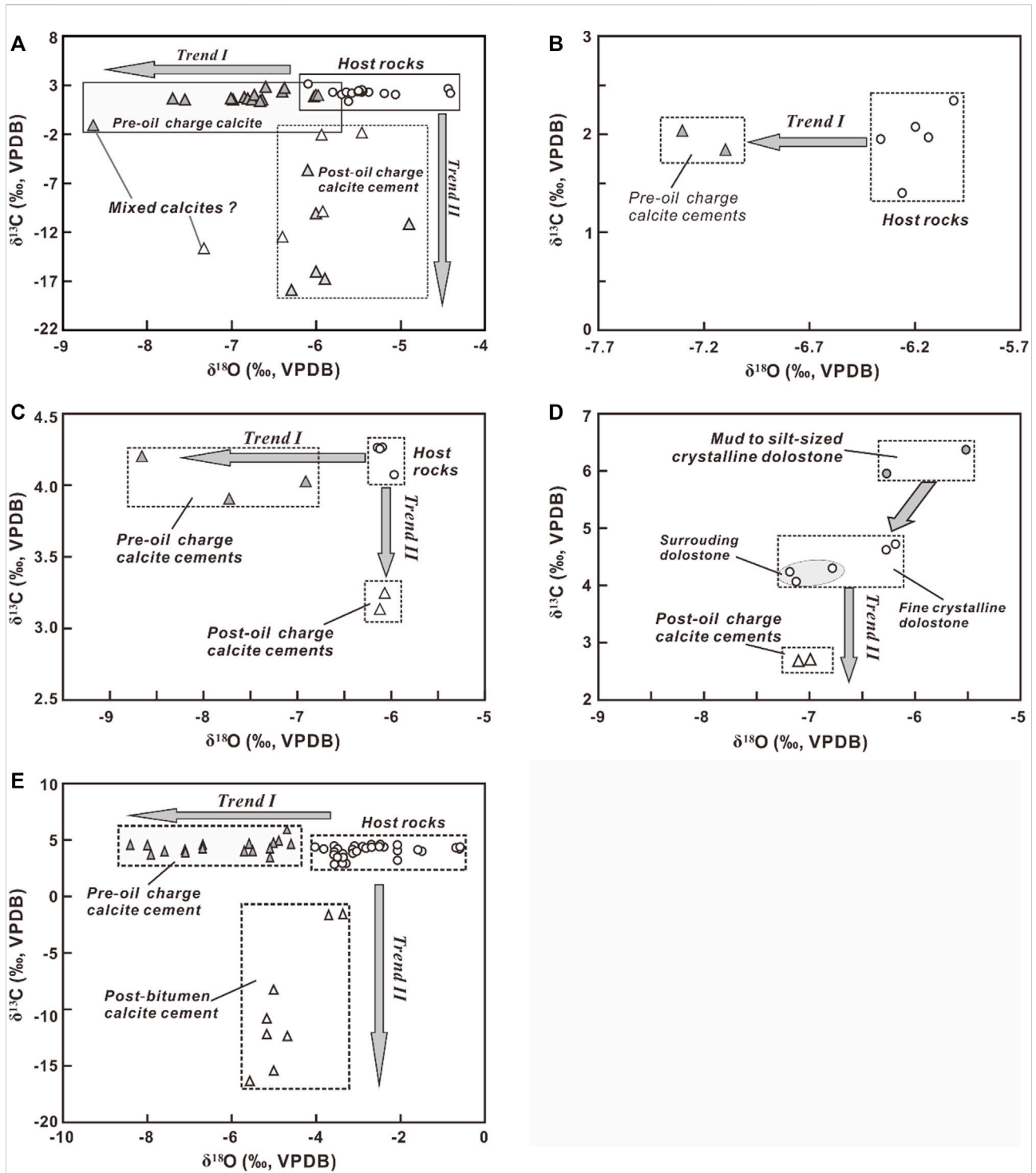
FIGURE 6
Oxygen and carbon isotope compositions of the pre and post-oil charge calcite cements in the Changxing and Feixianguan formations from the Puguang gas field **(A)**, Yuanba **(B)**, Fuling **(C)**, and Jiannan **(D)** gas fields. The rectangles show the ranges of data of different carbonate phases. The data (black open diamonds in figure A) are from Zhu et al. (2005) and represent the calcites that partially replaced anhydrite during TSR in the northeastern Sichuan Basin. Stable isotope compositions of calcites and host rocks from the Smackover Formation **(E)** were also present (Heydari and Moore, 1989) for comparison.

approximately 2 km in the southern United States up to about eight‰ SMOW (Moldovanyi et al., 1993). Furthermore, with increasing temperatures, the $\delta^{18}O$ values of pore waters become more positive (Swart et al., 2016). It seems that the relatively high $\delta^{18}O$ values of the post-oil charge cements may reflect precipitation from such ^{18}O-enriched fluids (Heydari and Moore, 1989). However, the highly temperature-dependent isotopic fractionation can promote calcite becoming much more depleted in $\delta^{18}O$ values, even if the calcites precipitated from pore fluids with heavy oxygen isotopic composition (Moore, 2001). The oxygen isotope composition of the fluid from which the calcite precipitated can be assessed based on cement $\delta^{18}O$ values and associated precipitation temperatures from fluid inclusions. Using the method of Friedman and O'Neil (1977), the average $\delta^{18}O$ value of -6.3‰ VPDB and the average temperatures of 150°C for calcites in the study area, the fluid for the post-oil charge calcite cements is calculated to have the $\delta^{18}O$ value of 11.5‰ SMOW, a quite positive $\delta^{18}O$ value for a sedimentary formation water (Longstaffe, 1989). Moreover, this ^{18}O-enriched fluid is expected to have $\delta^{13}C$ values similar to the host carbonate rocks, which is opposite to the fact of the most depleted $\delta^{13}C$ values of precipitated calcites relative to the host rocks (Figures 6A,C,D). Therefore, some other processes must be involved in the precipitation of the high $\delta^{18}O$ TSR-related calcites that would offset the high temperature effect of mineral-water fractionation.

Gases produced from carbonate reservoirs in the northeastern Sichuan Basin have the H_2S concentrations from about 2% in dolostone reservoirs of the northern Jiannan gas field to ~13% in the Fuling gas field, and about 16% in the Puguang gas field. The high H_2S concentrations are attributed to thermochemical sulfate reduction (TSR), which has been intensively investigated in the northeastern Sichuan Basin (e.g., Cai et al., 2003; Li et al., 2005; Zhu et al., 2005, 2014; Hao et al., 2008, 2015; Liu et al., 2013, 2014). The post-oil charge calcite cements in the study area commonly occur with solid bitumens (Figures 3B–F; Figures 4E,G), and the T_h values of fluid inclusions in these calcites roughly correspond to the range of temperatures for TSR during which the oxidation of hydrocarbons is usually accompanied by calcite precipitation (e.g., Machel, 2001). In addition, the lower $\delta^{13}C$ values of the TSR-related calcites, compared with host rocks, also reflect the contribution of organic carbon. The $\delta^{18}O$ and $\delta^{13}C$ values of TSR-related calcites in the Puguang gas field are comparable to those of calcites associated with anhydrite or partially replaced anhydrite during TSR (Zhu et al., 2005, Figure 6A), also suggesting the controls of TSR on the ^{18}O-enriched calcite precipitation. Some calcite samples that plot between the two trends may represent the mixed origin (Figure 6A). Therefore, the TSR-related calcites were closely associated with TSR.

Model for oxygen isotope behavior during TSR

TSR is a reaction between sulfate and hydrocarbons at temperature of greater than 100–140°C, and the simplified geochemical reaction can be expressed in the following (Machel et al., 1995; Machel, 2001):
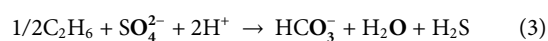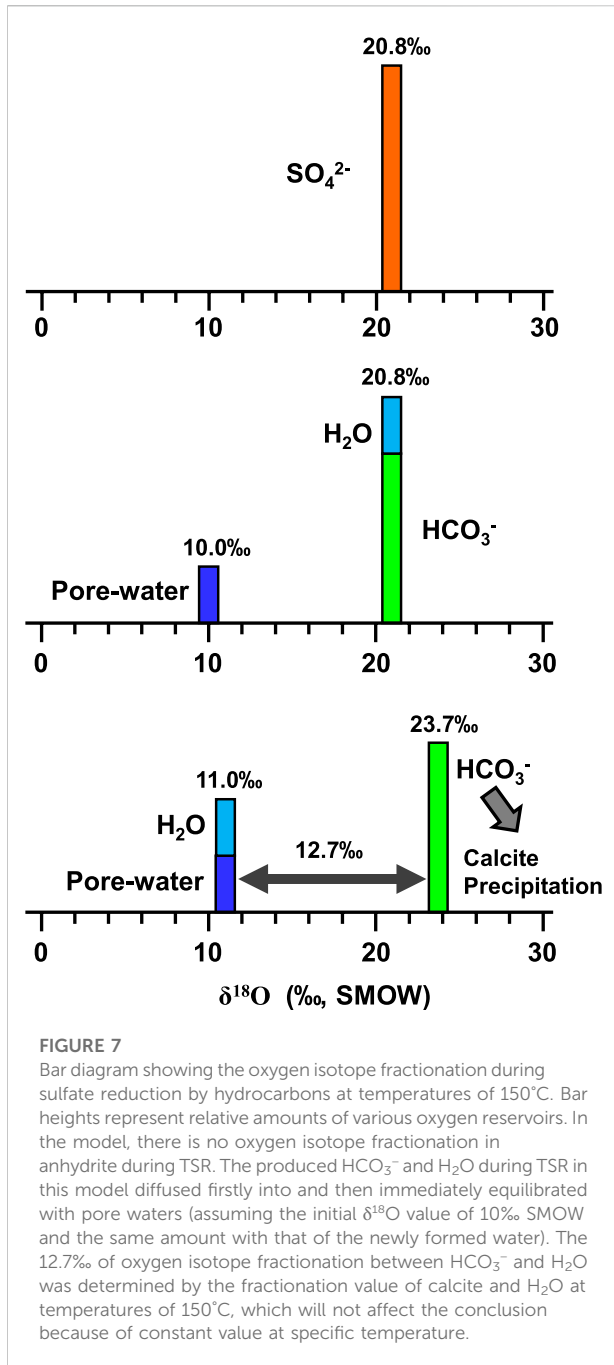
$$nCaSO_4 + C_nH_{2n+2} \ (hydrocarbons) \rightarrow nCaCO_3 + H_2S + nH_2O + solid \ bitumen \quad (1)$$
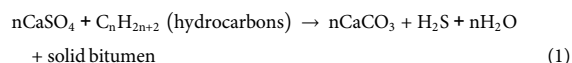
During TSR, the carbon generated from hydrocarbon oxidation is expected to have low $\delta^{13}C$ values, which is responsible for the ^{13}C depletion in the TSR-related calcites in the study area. Simultaneously, three oxygens liberated from the reduction of one SO_4^{2-} ion are incorporated into calcites (anhydrite-related calcite), leaving one oxygen to form water (anhydrite-related water) (Worden and Smalley, 1996). Thus, the oxygen isotope compositions of the anhydrite-related calcite ($\delta^{18}O_{anh\text{-}calcite}$) and water ($\delta^{18}O_{anh\text{-}water}$) depend largely on the $\delta^{18}O$ of the reduced anhydrite (Worden and Smalley, 1996). Assuming no oxygen isotope fractionation during TSR, the $\delta^{18}O_{anh\text{-}water}$ and $\delta^{18}O_{anh\text{-}calcite}$ can be calculated by the following equations (Worden and Smalley, 1996):

$$\delta^{18}O_{anh-calcite} = \delta^{18}O_{anhydrite} + 1/4\left[\left(2.78 \times 10^6/T^2\right) - 2.89\right] \quad (2)$$

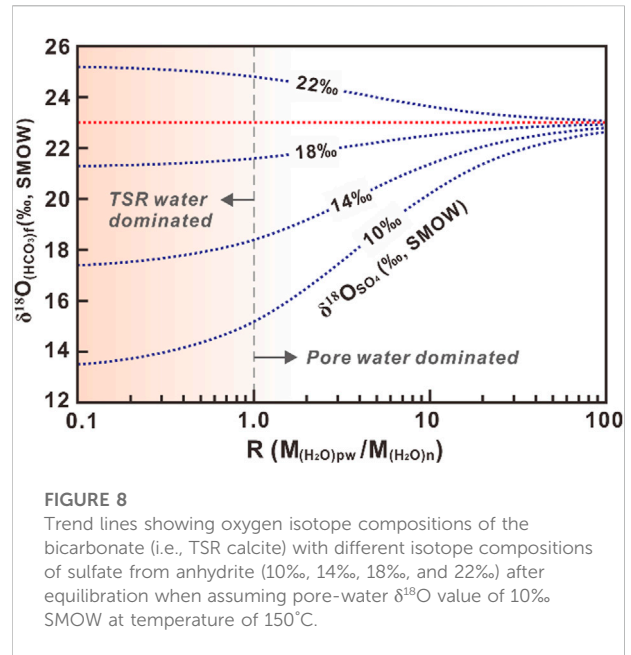The $\delta^{18}O$ values of anhydrites from the Feixianguan dolostones in the northeastern Sichuan Basin range from 16.4‰ to 23.1‰ SMOW with an average value of 18.6‰ SMOW (Table 2). Using an average T_h value of 150°C as the temperature for the formation of the calcite as an example, the anhydrite-related calcite has the $\delta^{18}O_{calcite}$ values from -11.0‰ to -4.5‰ V-PDB (average -8.9‰ V-PDB), less than the average value of the TSR-related calcites (-6.3‰ V-PDB) in the study area. In addition, the difference between theoretical value and measured data also exist in some other areas, such as the Smackover Formation discussed by Heydari and Moore (1989). Taking the $\delta^{18}O$ value of 14‰ SMOW as the Upper Jurassic anhydrite (Claypool et al., 1980; Dworkin and Land, 1994) and 150°C–200°C as a main range of formation temperatures for calcites, the anhydrite-related calcite has the $\delta^{18}O_{calcite}$ values of 16.4‰~17.2‰ SMOW (-14‰~-13.3‰ V-PDB), which are significantly lower than the measured $\delta^{18}O$ values (-5.6‰~-3.0‰ V-PDB) of the TSR calcites (Figure 6E) (Heydari and Moore, 1989). This implies pore waters in carbonate reservoirs may significantly affect the oxygen isotope compositions of the calcites during TSR.

A model is proposed for $\delta^{18}O$ of calcite formed under TSR conditions that is similar to that in Sass (1991) that accounts for the initial of anhydrite and pore water interactions with the host rock. Using C_2H_6 for example, its oxidation by sulfate ions at elevated temperatures can be expressed as (modified from Machel et al., 1995):

$$1/2C_2H_6 + SO_4^{2-} + 2H^+ \rightarrow HCO_3^- + H_2O + H_2S \quad (3)$$

FIGURE 7
Bar diagram showing the oxygen isotope fractionation during
sulfate reduction by hydrocarbons at temperatures of 150°C. Bar
heights represent relative amounts of various oxygen reservoirs. In
the model, there is no oxygen isotope fractionation in
anhydrite during TSR. The produced HCO_3^- and H_2O during TSR in
this model diffused firstly into and then immediately equilibrated
with pore waters (assuming the initial $\delta^{18}O$ value of 10‰ SMOW
and the same amount with that of the newly formed water). The
12.7‰ of oxygen isotope fractionation between HCO_3^- and H_2O
was determined by the fractionation value of calcite and H_2O at
temperatures of 150°C, which will not affect the conclusion
because of constant value at specific temperature.

As discussion above, if no oxygen isotope fractionation occurs
during TSR (Worden and Smalley, 1996), the newly formed
water and the bicarbonate have same $\delta^{18}O$ value, equal to isotope
compositions of the sulfate (i.e., $\delta^{18}O_{(HCO3)n} = \delta^{18}O_{(H2O)n} = \delta^{18}O_{SO4}$), and immediately diffused into pore waters in
reservoirs. Thus, the diagenetic system consists of three
oxygen reservoirs, including pore water ($M_{(H2O)pw}$), the newly
formed water ($M_{(H2O)n}$) and the bicarbonate (M_{HCO3}), and has
weighted-average isotope composition ($\delta^{18}O_{AV}$):

FIGURE 8
Trend lines showing oxygen isotope compositions of the
bicarbonate (i.e., TSR calcite) with different isotope compositions
of sulfate from anhydrite (10‰, 14‰, 18‰, and 22‰) after
equilibration when assuming pore-water $\delta^{18}O$ value of 10‰
SMOW at temperature of 150°C.

$$\delta^{18}O_{AV} = \left[\left(M_{(H2O)pw} \cdot \delta^{18}O_{(H2O)pw} + M_{(H2O)n} \cdot \delta^{18}O_{(H2O)n} \right. \right.$$
$$\left. \left. + M_{HCO3} \cdot \delta^{18}O_{(HCO3)n} \right) \right] / \left(M_{(H2O)pw} + M_{(H2O)n} \right.$$
$$\left. + M_{HCO3} \right) \qquad (4)$$

After equilibration, the final oxygen isotope compositions of the
H_2O ($\delta^{18}O_{(H2O)f}$) and bicarbonate ($\delta^{18}O_{(HCO3)f}$) have the
fractionation $\delta^{18}O_{(HCO3)f} = \delta^{18}O_{(H2O)f} + 12.7$ at 150°C. The
average $\delta^{18}O_{AV}$ ratio of the system can now be expressed as:

$$\delta^{18}O_{AV} = \left[\left(M_{(H2O)pw} + M_{(H2O)n} \right) \cdot \delta^{18}O_{(H2O)f} + M_{HCO3} \cdot \delta^{18}O_{(HCO3)f} \right] / \left(M_{(H2O)pw} + M_{(H2O)n} + M_{HCO3} \right)$$
$$(5)$$

Based on the Eq. 3, the oxygen ions (in moles) in bicarbonate
equals three times that of the newly formed water ($M_{HCO3} =
3M_{(H2O)n}$). If the ratio between the masses of original pore water
and the newly formed water is defined as R ($R = M_{(H2O)pw}/
M_{(H2O)n}$), equating expressions four and five results in:

$$\delta^{18}O_{(HCO3)f} = \left[4\delta^{18}O_{SO4} + R\delta^{18}O_{(H2O)pw} + 12.7(1 + R) \right] / (R + 4)$$
$$(6)$$

Therefore, the oxygen isotope composition of the calcite
precipitated (i.e., bicarbonate) during TSR would not only
depend on the isotope compositions of the anhydrite, but also
the $\delta^{18}O$ ratios and amounts of the pore water residue in
carbonate reservoirs (Figure 7).

Oxygen isotope behavior during TSR

TSR calcites (e.g., the TSR-related calcites in this study) are
very common in deep carbonate reservoirs worldwide, such as in
the Permian Khuff Formation in the Abu Dhabi (Worden et al.,

1996), the Smackover Formation in the Mississippi salt basin (Heydari and Moore, 1989), and the Lower Triassic Feixianguan Formation in the Sichuan Basin (Huang et al., 2012). Geochemical data in this study show that some calcite cements have $\delta^{18}O$ values significantly lower than that of host rocks, while others show values close to host rocks (Figure 6).

The oxygen isotope data for sulfate from marine evaporates show a range of about 10‰~22‰ SMOW (Claypool et al., 1980), and waters associated with marine evaporates could attain $\delta^{18}O$ of up to 10‰ SMOW (Knauth and Beeunas, 1986). For example, following the Eq. 6, and using the pore-water $\delta^{18}O_{(H2O)pw}$ of 10‰ SMOW, the trend lines for bicarbonate $\delta^{18}O_{(HCO3)f}$ values with different $\delta^{18}O_{SO4}$ of anhydrite can be obtained at reaction temperature of 150℃ (Figure 8). Although different trend lines could be generated using different isotope compositions of the pore water and reaction temperatures, the basic principal is similar.

Generally, TSR has two opposing effects on the oxygen isotope compositions of calcites, depending on initial anhydrite $\delta^{18}O$ value. The cross over point where the two effects balance is about 19.5‰ SMOW in this model (Figure 8). Thus, the calcites, such as those in this study, have heavier $\delta^{18}O$ values than that directly precipitated from pore waters, when the reactant anhydrites have $\delta^{18}O$ values greater than about 19.5‰ SMOW. Considering the boundary value of $\delta^{18}O$ greater than most Phanerozoic anhydrites, most sulfate reduction tends to lower $\delta^{18}O$ values of calcites during TSR (Figure 8). In addition, if the initial water saturation in reservoirs is low (R<1), the volume of water resulting from TSR is less than that of the pore waters. With R decreasing, the $\delta^{18}O$ values of the calcites decrease (Figure 8). Under such circumstances, the oxygen isotope composition of the calcite precipitated during TSR depends on isotope compositions of the initial anhydrite at specific temperature. If TSR occurs in reservoirs with high water saturations or in water-oil/gas transition zones, the influence of pore water becomes obvious. This may be the reason why TSR calcites from the Smackover Formation in Mississippi salt basin (Heydari and Moore, 1989) have heavier $\delta^{18}O$ values, even though the reactant anhydrites have $\delta^{18}O$ values of only about 14‰ SMOW.

Conclusion

Compared to the host carbonate rocks, the burial calcite cements from the Changxing and Feixianguan formations in the Sichuan Basin show two distinct trends in carbon and oxygen-isotope compositions. The decreasing trend in $\delta^{18}O$ ratios of the pre-TSR calcites reflects precipitation at increasing temperatures with carbon isotope compositions buffered mainly by host rocks. In contrast, the TSR-related calcites, despite precipitated at higher temperatures than the pre-TSR calcites, have heavier $\delta^{18}O$ values close to, or overlapped partly with those of host rocks. The lighter $\delta^{13}C$ values of the TSR-

related calcites relative to the host rocks, as well as close association with solid bitumen, suggest a contribution of organic carbon derived from thermochemical sulfate reduction, a process that not only provides the light carbon, but also supplies oxygen for calcites at high temperatures. Based on the model established, the oxygen isotope compositions of the TSR calcites are a function of the isotope compositions and amounts of the initial anhydrite and pore water residue in carbonate reservoirs. TSR show two opposing effects on the $\delta^{18}O$ values of calcites, depending on the $\delta^{18}O$ ratios of the initial anhydrite involved. The reduction of anhydrite with relatively low $\delta^{18}O$ values causes the $\delta^{18}O$ of calcite lower than theoretical values of that directly precipitated from pore waters. The heavy oxygen isotope compositions of calcites formed during TSR are not only attributed to the ^{18}O-enriched pore water resulting from extensive water-rock interaction, but also probably due to the involvement of anhydrite with high $\delta^{18}O$ values.

Data availability statement

The original contributions presented in the study are included in the article/supplementary material, further inquiries can be directed to the corresponding author.

Author contributions

WG, HF, and ZH contributed to conception and design of the study. WG organized the database. WG and LP performed the analysis. WG wrote the first draft of the manuscript. All authors contributed to manuscript revision, read, and approved the submitted version.

Funding

Acknowledgments

Conflict of interest

The authors declare that the research was conducted in the absence of any commercial or financial relationships that could be construed as a potential conflict of interest.

Publisher's note

All claims expressed in this article are solely those of the authors and do not necessarily represent those of their affiliated organizations, or those of the publisher, the editors and the reviewers. Any product that may be evaluated in this article, or claim that may be made by its manufacturer, is not guaranteed or endorsed by the publisher.

References

Allan, J. R., and Wiggins, W. D. (1993). Dolomite reservoirs: Geochemical techniques for evaluating origin and distribution. *AAPG Contin. Educ. Course Note Ser.* 36, 129. doi:10.1306/CE36576

Cai, C., Worden, R. H., Bottrell, S. H., Wang, L., and Yang, C. (2003). Thermochemical sulphate reduction and the generation of hydrogen sulphide and thiols (mercaptans) in Triassic carbonate reservoirs from the Sichuan Basin, China. *Chem. Geol.* 202, 39–57. doi:10.1016/s0009-2541(03)00209-2

Claypool, G. E., Holser, W. T., Kaplan, I. R., Sakai, H., and Zak, I. (1980). The age curves of sulfur and oxygen isotopes in marine sulfate and their mutual interpretation. *Chem. Geol.* 28, 199–260. doi:10.1016/0009-2541(80)90047-9

Dworkin, S. I., and Land, L. S. (1994). Petrographic and geochemical constraints on the formation and diagenesis of anhydrite cements, Smackover sandstones, Gulf of Mexico. *J. Sediment. Res.* 64, 339–348. doi:10.1306/D4267D98-2B26-11D7-8648000102C1865D

Fouke, B. W., and Rakovan, J. (2001). An integrated cathodoluminescence video-capture microsampling system. *J. Sediment. Res.* 71, 509–513. doi:10.1306/2dc4095c-0e47-11d7-8643000102c1865d

Friedman, I., and O'Neil, J. R. (1977). "Compilation of stable isotope fractionation factors of geochemical interest," in *Data of Geochemistry*. Editor M. Fleischer. 6th ed. (Washington: USGS Professional. Paper 440-KK), 11.

Hao, F., Guo, T., Zhu, Y., Cai, X., Zou, H., and Li, P. (2008). Evidence for multiple stages of oil cracking and thermochemical sulfate reduction in the Puguang gas field, Sichuan Basin, China. *Am. Assoc. Pet. Geol. Bull.* 92, 611–637. doi:10.1306/01210807090

Hao, F., Zhang, X., Wang, C., Li, P., Guo, T., Zou, H., et al. (2015). The fate of CO_2 derived from thermochemical sulfate reduction (TSR) and effect of TSR on carbonate porosity and permeability, Sichuan Basin, China. *Earth-Science Rev.* 141, 154–177. doi:10.1016/j.earscirev.2014.12.001

Heydari, E., and Moore, C. H. (1989). Burial diagenesis and thermochemical sulfate reduction, Smackover Formation, southeastern Mississippi salt basin. *Geol.* 17, 1080–1084. doi:10.1130/0091-7613(1989)017<1080:bdatsr>2.3.co;2

Huang, S., Huang, K., Li, Z., Fan, M., Xu, E., and Lü, J. (2012). TSR-derived authigenic calcites in Triassic dolomite, NE Sichuan basin, China - a case study of well HB-1 and well L-2. *J. Earth Sci.* 23, 88–96. doi:10.1007/s12583-012-0235-8

Li, J., Xie, Z. Y., Dai, J. X., Zhang, S. C., Zhu, G. Y., and Liu, Z. L. (2005). Geochemistry and origin of sour gas accumulations in the northeastern Sichuan Basin, SW China. *Org. Geochem.* 36, 1703–1716. doi:10.1016/j.orggeochem.2005.08.006

Li, P., Hao, F., Guo, X., Zou, H., Zhu, Y., Yu, X., et al. (2016). Origin and distribution of hydrogen sulfide in the Yuanba gas field, Sichuan Basin, Southwest China. *Mar. Petroleum Geol.* 75, 220–239. doi:10.1016/j.marpetgeo.2016.04.021

Liu, Q. Y., Worden, R. H., Jin, Z. J., Liu, W. H., Li, J., Gao, B., et al. (2014). Thermochemical sulphate reduction (TSR) versus maturation and their effects on hydrogen stable isotopes of very dry alkane gases. *Geochimica Cosmochimica Acta* 137, 208–220. doi:10.1016/j.gca.2014.03.013

Liu, Q. Y., Worden, R. H., Jin, Z. J., Liu, W. H., Li, J., Gao, B., et al. (2013). TSR versus non-TSR processes and their impact on gas geochemistry and carbon stable isotopes in Carboniferous, Permian and Lower Triassic marine carbonate gas reservoirs in the Eastern Sichuan Basin, China. *Geochimica Cosmochimica Acta* 100, 96–115. doi:10.1016/j.gca.2012.09.039

Ma, Y. S., Zhang, S. C., Guo, T. L., Zhu, G. Y., Cai, X. Y., and Li, M. W. (2008). Petroleum geology of the Puguang sour gas field in the Sichuan Basin, SW China. *Mar. Petroleum Geol.* 25, 357–370. doi:10.1016/j.marpetgeo.2008.01.010

Machel, H. G. (2001). Bacterial and thermochemical sulfate reduction in diagenetic settings - old and new insights. *Sediment. Geol.* 140, 143–175. doi:10.1016/s0037-0738(00)00176-7

Machel, H. G., Krouse, H. R., and Sassen, R. (1995). Products and distinguishing criteria of bacterial and thermochemical sulfate reduction. *Appl. Geochem.* 10, 373–389. doi:10.1016/0883-2927(95)00008-8

Mangenot, X., Gasparrini, M., Rouchon, V., and Bonifacie, M. (2018). Basin-scale thermal and fluid flow histories revealed by carbonate clumped isotopes (Δ47)– Middle Jurassic carbonates of the Paris Basin depocentre. *Sedimentology* 65, 123–150. doi:10.1111/sed.12427

Moldovanyi, E. P., Walter, L. M., and Land, L. S. (1993). Strontium, boron, oxygen, and hydrogen isotope geochemistry of brines from basal strata of the Gulf-Coast sedimentary basin, USA. *Geochimica Cosmochimica Acta* 57, 2083–2099. doi:10.1016/0016-7037(93)90095-e

Moore, C. H. (2001). *Carbonate reservoirs porosity evolution and diagenesis in a sequence stratigraphic framework*. Amsterdam: Elsevier, 444.

Morad, S. (2009). *Carbonate cementation in sandstones: Distribution patterns and geochemical evolution*. John Wiley & Sons, 514.

Sass, E., Bein, A., and Almogi-Labin, A. (1991). Oxygen-isotope composition of diagenetic calcite in organic-rich rocks: Evidence for ^{18}O depletion in marine anaerobic pore water. *Geol.* 19, 839–842. doi:10.1130/0091-7613(1991)019<0839:oicodc>2.3.co;2

Schneidermann, N., and Harris, P. M. (1985). Carbonate cements: Based on a symposium sponsored by the society of economic paleontologists and mineralogists. *SEPM Soc. Sediment.* 36, 371. doi:10.2110/pec.85.36

Swart, P. K., Cantrell, D. L., Arienzo, M. M., and Murray, S. T. (2016). Evidence for high temperature and ^{18}O-enriched fluids in the arab-D of the ghawar field, Saudi arabia. *Sedimentology* 63, 1739–1752. doi:10.1111/sed.12286

Wang, G. W., Chang, X. C., Yin, W., Li, Y., and Song, T. T. (2017). Impact of diagenesis on reservoir quality and heterogeneity of the Upper Triassic Chang 8 tight oil sandstones in the Zhenjing area, Ordos Basin, China. *Mar. Petroleum Geol.* 83, 84–96. doi:10.1016/j.marpetgeo.2017.03.008

Wang, G. W., Hao, F., Zhang, W. B., Zou, H. Y., and Li, P. P. (2022). Characterization and origin of micropores in tight gas grainstones of the lower triassic Feixianguan formation in the jiannan gas field, Sichuan Basin. *Mar. Petroleum Geol.* 139, 105609. doi:10.1016/j.marpetgeo.2022.105609

Wang, G. W., Li, P. P., Hao, F., Zou, H. Y., and Yu, X. Y. (2015b). Impact of sedimentology, diagenesis, and solid bitumen on the development of a tight gas grainstone reservoir in the Feixianguan formation, jiannan area, China: Implications for gas exploration in tight carbonate reservoirs. *Mar. Petroleum Geol.* 64, 250–265. doi:10.1016/j.marpetgeo.2015.02.045

Wang, G. W., Li, P. P., Hao, F., Zou, H. Y., and Yu, X. Y. (2015a). Origin of dolomite in the third member of Feixianguan formation (lower triassic) in the jiannan area, Sichuan Basin, China. *Mar. Petroleum Geol.* 63, 127–141. doi:10.1016/j.marpetgeo.2015.01.019

Wei, G., Chen, G., Yang, W., Yang, Y., Hu, M., Zhang, L., et al. (2004). Sedimentary system of platformal trough of Feixianguan formation of lower triassic in northern Sichuan Basin and its evolution. *Acta Sedimentol. Sin.* 22, 254–260. doi:10.4236/ojg.2020.106029

Worden, R. H., and Smalley, P. C. (1996). H_2S-producing reactions in deep carbonate gas reservoirs: Khuff Formation Abu Dhabi. *Chem. Geol.* 133, 157–171. doi:10.1016/s0009-2541(96)00074-5

Zhu, G., Fei, A., Zhao, J., and Liu, C. (2014). Sulfur isotopic fractionation and mechanism for thermochemical sulfate reduction genetic H_2S. *Acta Petrol. Sin.* 30, 3772–3786.

Zhu, G., Zhang, S., Liang, Y., Dai, J., and Li, J. (2005). Isotopic evidence of TSR origin for natural gas bearing high H_2S contents within the Feixianguan Formation of the northeastern Sichuan Basin, southwestern China. *Sci. China Ser. D-Earth. Sci.* 48, 1960–1971. doi:10.1360/082004-147

Zou, H., Hao, F., Zhu, Y., Guo, T., Cai, X., Li, P., et al. (2008). Source rocks for the Puguang gas field, Sichuan Basin: Implication for petroleum exploration in marine sequences in South China. *Acta Geol. Sin.* 82, 477–486. doi:10.1111/j.1755-6724.2008.tb00598.x